



Colossal nonsaturating linear magnetoresistance in two-dimensional electron systems at a GaAs/(Al,Ga)As heterointerface

M. A. Aamir,^{1,*} Srijit Goswami,¹ Matthias Baenninger,² Vikram Tripathi,³ Michael Pepper,⁴ Ian Farrer,² David A. Ritchie,² and Arindam Ghosh¹

¹*Department of Physics, Indian Institute of Science, Bangalore 560 012, India*

²*Cavendish Laboratory, University of Cambridge, J.J. Thomson Avenue, Cambridge CB3 0HE, United Kingdom*

³*Department of Theoretical Physics, Tata Institute of Fundamental Research, Homi Bhabha Road, Mumbai 400005, India*

⁴*Department of Electrical and Electronic Engineering, University College, London WC1E 7JE, United Kingdom*

(Received 13 July 2012; published 24 August 2012)

Engineering devices with a large electrical response to magnetic field is of fundamental importance for a range of applications such as magnetic field sensing and magnetic read heads. We show that a colossal nonsaturating linear magnetoresistance (NLMR) arises in two-dimensional electron systems hosted in a GaAs/AlGaAs heterostructure in the strongly insulating regime. When operated at high source-drain bias, the magnetoresistance of our devices increases almost linearly with magnetic field, reaching nearly 10 000% at 8 T, thus surpassing many known nonmagnetic materials that exhibit giant NLMR. The temperature dependence and mobility analysis indicate that the NLMR has a purely classical origin, driven by nanoscale inhomogeneities. A large NLMR combined with small device dimensions makes these systems an attractive candidate for on-chip magnetic field sensing.

DOI: [10.1103/PhysRevB.86.081203](https://doi.org/10.1103/PhysRevB.86.081203)

PACS number(s): 72.20.My

In a nonmagnetic semiconductor, giant positive nonsaturating linear magnetoresistance (NLMR) can have either a classical¹⁻⁴ or quantum origin.^{5,6} The quantum NLMR, originally proposed by Abrikosov,^{5,6} is applicable in the extreme quantum limit where $\hbar\omega_c \gg E_F, k_B T$ (ω_c and E_F are the cyclotron frequency and Fermi energy, respectively). This criterion can be attained in a restricted class of materials which includes semimetals such as bismuth, or narrow band gap semiconductors with very low effective mass (e.g., InSb,³ graphene,⁷ and topological insulators⁸). The classical NLMR, on the other hand, is commonly observed in systems with an inhomogeneous carrier (and hence mobility) distribution.^{4,9} It is a purely geometric effect, where, in the presence of a transverse magnetic field, a misalignment between current paths and the externally applied bias mixes the off-diagonal components of the magnetoresistivity tensor, resulting in a NLMR. Several classically inhomogeneous conductors, most notably the mildly doped silver chalcogenides ($\text{Ag}_{2+\delta}\text{Se}$ or $\text{Ag}_{2+\delta}\text{Te}$)¹ and InSb polycrystals,³ display extremely large NLMR, where the inhomogeneity is associated with intrinsic disorder such as grain boundaries, dopant clustering, etc. Thus a handle on the disorder, both in magnitude and length scale, could yield a new class of high sensitivity magnetoresistive devices. However, achieving such a control in bulk materials is not a trivial task.

Two-dimensional electron systems (2DESs) in semiconductor multilayers, in particular doped GaAs/AlGaAs heterostructures, offer a material platform in which disorder can be tuned with great precision by using molecular beam epitaxy. At high carrier density, since the heterointerface is physically separated from the ionized dopants, it is a homogeneous medium which hosts high mobility electrons. Therefore, it is not expected to be a good candidate for exhibiting NLMR. This is confirmed by numerous magnetoresistance (MR) measurements in 2DESs, which are best studied in two limits. At high carrier densities, the MR of a 2DES is oscillatory in magnetic field (B) due to the Shubnikov-de Haas effect,

while at lower carrier densities, at the onset of localization, the MR increases exponentially with B due to variable range hopping.¹⁰ Clearly, studies in neither regime have thus far revealed a NLMR.

A 2DES, however, does become inhomogeneous when it is depleted by applying a strong negative gate voltage on a surface gate electrode.¹¹ This constitutes the backbone of our experiments in the following way: For a typical doped GaAs/AlGaAs heterostructure with spacer thickness d , the Coulomb potential from the randomly scattered ionized dopants forms the dominant component of disorder. This causes the conduction band minimum to fluctuate as a function of position [see Fig. 1(b)] with a correlation length of $\sim 2d$.¹²⁻¹⁴ In this regime, the 2DES disintegrates into small puddles of charge that often manifest in Coulomb blockade effects in mesoscopic devices.^{11,13,15} In essence, this increase in inhomogeneity arises due to the weakening of electrostatic screening of the background disorder potential landscape, causing the spatial fluctuations in carrier density to be of the same order as the carrier density itself. We show that such a strong density variation at the GaAs/AlGaAs interface does in fact give rise to a giant NLMR in a simple gate-tunable mesoscopic system.

Our experiments are carried out in strongly insulating 2DESs in the GaAs/AlGaAs heterostructure where we explore the magnetic response of the system as a function of gate voltage (V_g) and source-drain bias (V_{sd}). The heterostructures contain a δ -doped layer of Si dopants of doping density $2.5 \times 10^{12} \text{ cm}^{-2}$ placed 40 nm above the GaAs/AlGaAs interface. The 2DES lies 90 nm below the surface, with an as-grown mobility $\sim 300 \text{ m}^2/\text{Vs}$. The etched mesa and a surface gate define the effective geometry of the device. Here we present results from a $3 \mu\text{m} \times 7 \mu\text{m}$ device [see Figs. 1(a) and 1(b)], though similar devices on two separate wafers showed qualitatively similar results (see the Supplemental Material¹⁶). The gate is used to pinch off the device by application of a negative voltage, and the resulting conductance

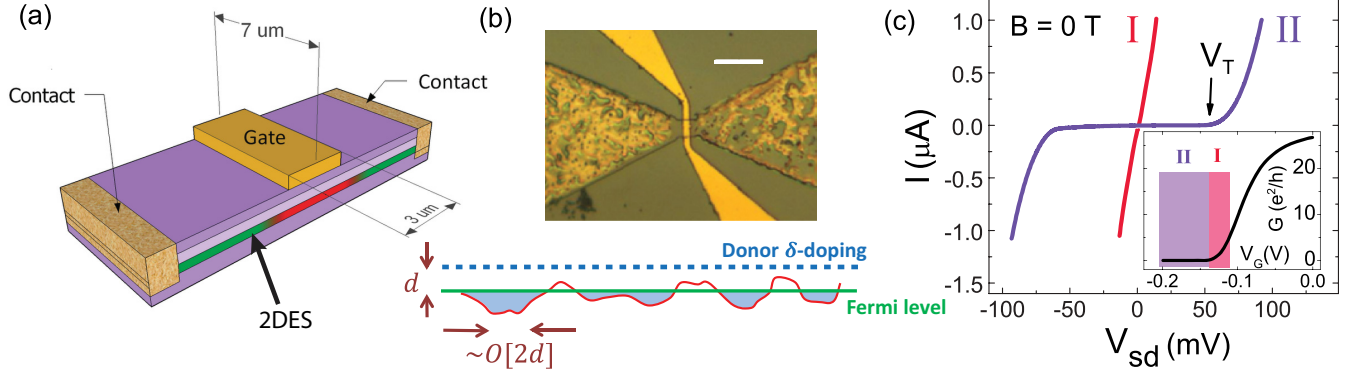


FIG. 1. (Color online) Device structure and characteristics. (a) Schematic of the device: The gate modulates the electron number density only in region of 2DES below it (highlighted red), thus defining the mesoscopic region of interest. (b) Top: Optical micrograph of the device. The scale bar is $20 \mu\text{m}$. Bottom: Potential landscape profile for the electrons at very low number density. (c) Inset: Equilibrium conductance as a function of the gate voltage. Region I represents the gate voltage just above the pinch-off (the point when equilibrium conductance becomes zero); region II represents another set of gate voltages below the pinch-off point. The main figure shows I - V_{sd} characteristics of the device for these two distinct regions at 0.3 K. The arrow indicates the threshold voltage V_T .

curve is shown in the inset of Fig. 1(c). Figure 1(c) shows I - V_{sd} characteristics at two values of V_g , representative of the two regions identified as regions I and II. Region I represents the onset of localization at linear conductance $G \sim e^2/h$, and has a reasonably ohmic I - V_{sd} . Region II, however, lies deep in the pinched-off regime where the 2DES is expected to become inhomogeneous. Here, we find the I - V_{sd} characteristics are strongly nonlinear with an insulating regime up to a threshold voltage V_T [indicated by an arrow in Fig. 1(c)], which increases monotonically as V_g is made increasingly negative (see the Supplemental Material¹⁶). Within this threshold, the current is immeasurably small ($<10^{-11}$ A), and conduction sets in rapidly only after the source-drain bias is increased beyond V_T . This rapid rise of current above threshold cannot be associated with avalanche breakdown that is common in semiconductors.^{17–19} This is because the applied electric fields are three orders of magnitude lower than the breakdown field in GaAs.¹⁸ The strong dependence of I - V_{sd} curves on magnetic field (to be discussed later) also eliminates self-heating effects as a cause for the rapidly rising current. In fact, a systematic analysis of the I - V_{sd} characteristics reveals that they follow a power law, characteristic of a disordered array of charge puddles^{20–26} (see the Supplemental Material¹⁶). This provides direct evidence that in region II the system is indeed highly inhomogeneous.

This inhomogeneity has a dramatic effect on the MR when subjected to a transverse magnetic field. At the onset of localization (prior to pinch-off), represented by region I in Fig. 1(c), the resistance R (obtained using equilibrium measurements) increases exponentially with B . As shown in Fig. 2(a), $R \sim \exp(B^2)$ at low B , which changes to $R \sim \exp(B)$ as B exceeds 2 T. These are characteristic features of hopping transport in the perturbative (low- B) and nonperturbative (high- B) regime, and recently studied in detail by some of us.¹⁰ In the sub-pinch-off regime, represented by region II, R was found to behave very differently. Most notably, its structure is highly sensitive to the magnitude of V_{sd} . To elucidate this, we define the dc magnetoresistance $R = R(V_{sd}, B) = V_{sd}/I(V_{sd}, B)$, and plot it as a function of B

for different values of V_{sd} in Fig. 2(b) [we carried out the same analysis with differential resistance $dV_{sd}/dI(V_{sd}, B)$, which did not yield a significantly different result]. Strikingly,

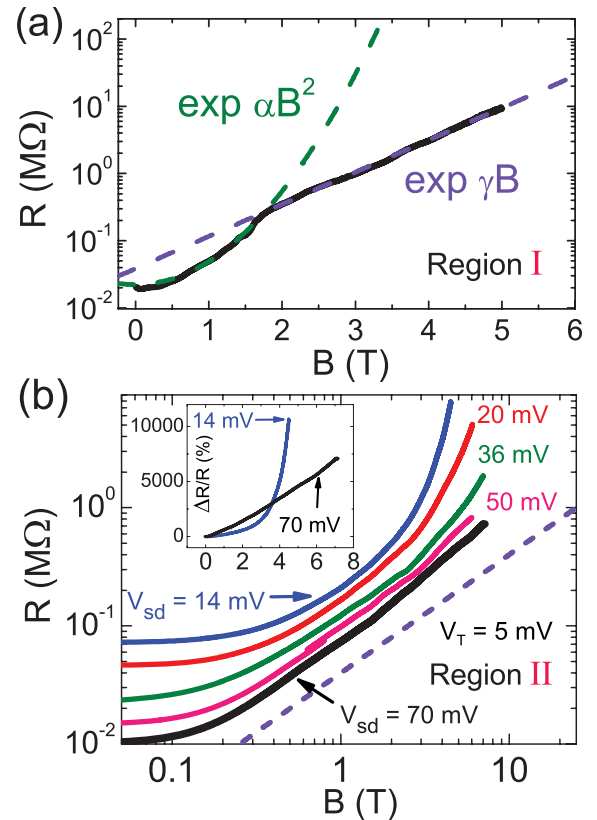


FIG. 2. (Color online) Magnetoresistance of the device. (a) MR of the sample for gate voltages above the pinch-off voltage (region I) obtained using ac lock-in measurements. (b) MR at different V_{sd} below the pinch-off point (region II). As source-drain is increased, the MR gradually transforms from a rapidly rising curve to a power law with exponent 1.1. The dashed line is $R \propto B$. Inset: Percentage change in resistance $\Delta R/R(\%)$ for two V_{sd} of 14 and 70 mV.

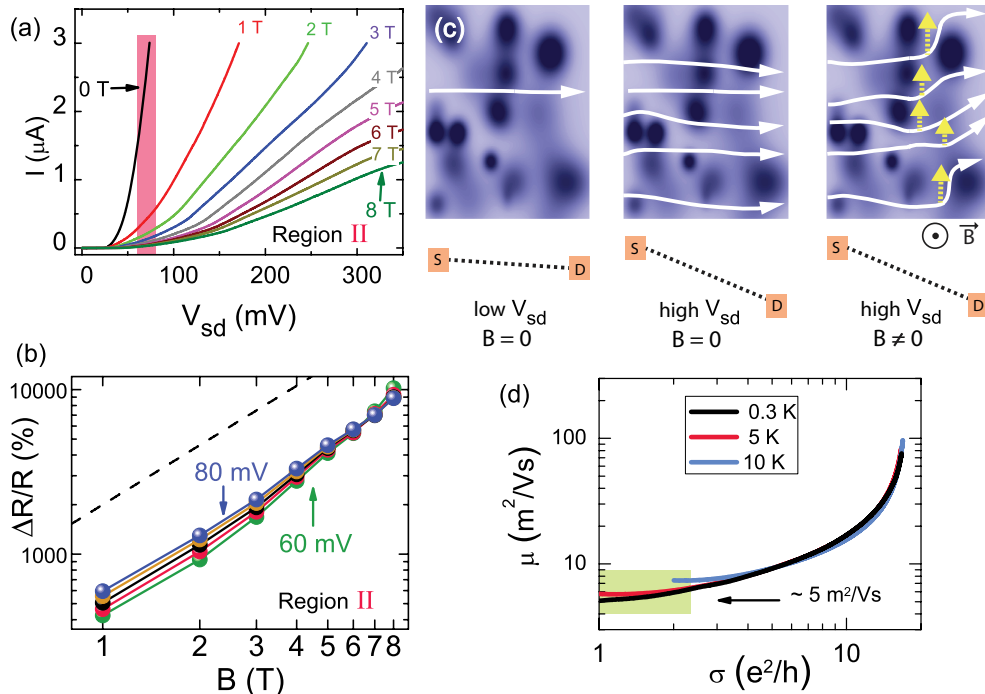


FIG. 3. (Color online) Source-drain bias dependence of the linear MR. (a) I - V_{sd} characteristics as a function of magnetic field from 0 to 8 T (in steps of 1 T) at 0.3 K (region II). (b) $\Delta R/R(\%)$ for different V_{sd} chosen from the shaded region of (a) (V_{sd} step size is 5 mV). The dashed line is $\Delta R/R \propto B^{1.2}$. (c) A schematic illustrating the possible origin of NLMR: The light (dark) regions represent areas of high (low) carrier number density. White arrows represent the current paths. Left: At low V_{sd} , there is only one or very few current channels. Middle: For high V_{sd} , the number of current paths proliferates rapidly. Right: On applying a perpendicular magnetic field at high V_{sd} , the plurality of the paths in the disordered medium gives rise to nontrivial current trajectories which have a significant transverse component (highlighted by dotted yellow arrows) that mixes the Hall contribution into the longitudinal MR, thus giving rise to NLMR. (d) The mobility (calculated using Drude's formula) as a function of the conductivity of the device at 0.3, 5, and 10 K.

the variation in R weakens with increasing V_{sd} , and for sufficiently high $V_{sd} \gg V_T$ ($V_T \approx 5$ mV at $V_g = -0.174$ V, $B = 0$ T), R increases linearly with B . In order to quantify the change in R , we evaluate the percentage change

$$\frac{\Delta R}{R}(\%) = \frac{[R(V_{sd}, B) - R(V_{sd}, 0)]}{R(V_{sd}, 0)} \times 100.$$

This quantity has been plotted for the two extremal V_{sd} in the inset of Fig. 2(b), and clearly shows that even the percentage change in R has transformed from a rapidly rising exponential curve to a strikingly linear form.

To study this more systematically, we look at the evolution of the I - V_{sd} characteristics as B is increased from 0 to 8 T. We have chosen a gate voltage corresponding to $V_T \approx 30$ mV (see the Supplemental Material¹⁶). Figure 3(a) shows that a nonzero B suppresses the current drastically, leading to a positive MR that increases monotonically with B . Within the experimentally achievable B (8 T) the measured R did not show any sign of saturation. We have evaluated $\Delta R/R(\%)$ (as defined above) for a few values of V_{sd} above V_T [the range is highlighted in Fig. 3(a)]. As shown in Fig. 3(b), the MR in our mesoscopic 2DES reaches almost 10 000% at $B = 8$ T for $V_{sd} = 80$ mV. As expected from Fig. 2(b), the MR becomes nearly linear with increasing V_{sd} . The dashed line in Fig. 3(b) represents $\Delta R/R \propto B^{1.2}$.

The inherent inhomogeneity in charge distributions and a parabolic dispersion relation for the carriers makes the clas-

sical model for NLMR proposed by Parish and Littlewood^{4,9} particularly applicable in our devices. The findings in Ref. 4 followed from a numerical simulation of an equivalent node-link network model. Using the same physical principles, we have presented in the Supplemental Material¹⁶ an alternate theoretical analysis for NLMR in a 2D inhomogeneous conductor, which augments existing theoretical descriptions.^{4,9,27–31} The classical model requires current flow from source to drain to occur via multiple channels in order to realize the nontrivial magnetic response of NLMR. The process by which NLMR arises in our devices is depicted schematically in Fig. 3(c). At low V_{sd} (left schematic), there are very few electron channels for conduction and are not sufficient in number to give rise to NLMR. However, a high V_{sd} (middle schematic) opens up many more conduction channels. This is similar to the nonequilibrium transport in a disordered array of quantum dots where the multiplication of paths is directly connected to the conduction threshold.²⁶ A perpendicular magnetic field distorts these current paths, which form nontrivial trajectories through the inhomogeneous medium,⁴ resulting in a substantial transverse component (dotted arrows in the right schematic). This allows a significant mixing of the off-diagonal components in the magnetoresistivity tensor, thus leading to the NLMR. This qualitative picture allows us to intuitively understand why we observe NLMR only at high values of V_{sd} . We note that studies on mildly doped Si also reported a seemingly similar dependence of the quantity

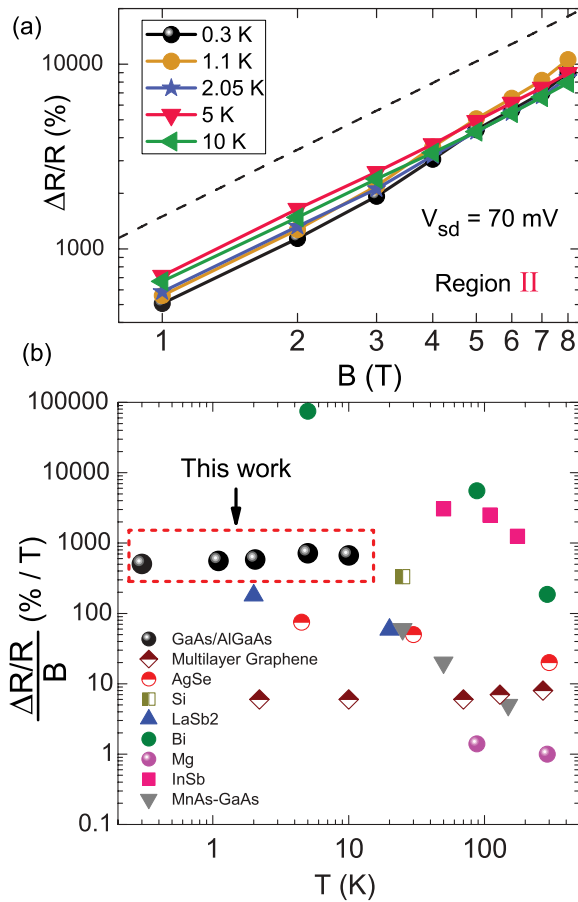


FIG. 4. (Color online) Temperature dependence of linear MR. (a) $\Delta R/R$ at different temperatures: 0.3, 1.1, 2.05, 5, and 10 K for region II. The dashed line represents $\Delta R/R \propto B^{1.2}$. (b) Comparison of MR of our device (highlighted by the dashed box) with other nonmagnetic materials which have linear MR: $\text{Ag}_{2+\delta}\text{Se}$,¹ multilayer graphene,⁷ bulk Si,² InSb,³ LaSb₂,³² Bi,^{33,34} Mg,³⁵ and MnAs-GaAs composite.³⁶

$\Delta R/R$ on source-drain bias.² However, the NLMR there was connected to an inhomogeneous electric field in the presence of space-charge injection. This scenario is certainly not applicable in our case since the bias applied in our experiments is significantly lower than that required to induce bulk semiconductor transport.^{18,19}

An important question that must be addressed is whether the inhomogeneity in our systems can quantitatively explain the magnitude and field scales associated with the observed NLMR. Being a δ -doped heterostructure, the dopant atoms are located at roughly the same distance from the 2DES, and

hence the amplitude of conduction band fluctuations is unlikely to vary widely from one location to another. Therefore, it is not unreasonable to assume that the width of mobility distribution $\Delta\mu$ is smaller than the average mobility $\langle\mu\rangle$ among the charge puddles. In such a case, the classical model predicts a quadratic to linear MR transition at $B \sim \langle\mu\rangle^{-1}$, with $\Delta R(B)/R = c\langle\mu\rangle B$ in the linear regime³⁰ (c is a constant of order unity that depends on the details of mobility distribution). From Fig. 3(b), we find that $\Delta R(B)/R(0)B \approx 5 \text{ T}^{-1}$, which is consistent with the fact that the transition to linear MR occurs around 0.1–0.2 T [see Fig. 2(b)]. Moreover, a rough estimate of $\langle\mu\rangle$ can be obtained from the mobility of the device at the onset of localization which is usually identified by conductivity $\rightarrow e^2/h$ for a 2DES. Below this conductivity, the system starts becoming disintegrated and incompressible.³⁷ In Fig. 3(d) we have shown the variation in the Drude mobility of our device as a function of its conductivity for a few temperatures. The limiting mobility at the onset of localization is about $5 \text{ m}^2/\text{Vs}$, which is in good order-of-magnitude agreement with $\Delta R(B)/R(0)B$. Interestingly, $\langle\mu\rangle$ is not a strong function of temperature in our heterostructures, at least up to 10 K, presumably because electron-phonon interactions contribute less to the resistivity than elastic residual scattering. This should also carry over to a weak temperature dependence of the NLMR. Figure 4(a) shows that, indeed, the NLMR retains roughly the same magnitude for a temperature range from 0.3 to 10 K, thus spanning nearly two orders of magnitude.

Finally, we compare the sensitivity of the disordered GaAs/AlGaAs heterostructure with other nonmagnetic systems that exhibit NLMR. The sensitivity of our device is extracted from its value at 1 T in Fig. 4(a) and is an increasing function of V_{sd} (see the Supplemental Material¹⁶). The highest value that is directly observed is about 500% per T at $V_{sd} = 70 \text{ mV}$. In Fig. 4(b) we have compiled the reported values of $\Delta R(B)/R(0)B$ (in percentage per T) from a wide variety of nonmagnetic semiconductors and semimetals. Clearly, the sensitivity of the GaAs/AlGaAs system is comparable to existing nonmagnetic materials. This virtue, along with the electrical tunability of the MR, makes mesoscopic GaAs/AlGaAs heterostructures unique in comparison to other material systems. In fact, more efficient and clever gating assemblies could possibly achieve an even higher sensitivity and form a new class of magnetoresistive sensors.

We would like to acknowledge support from the Department of Science and Technology, Government of India and UKIERI. S.G. thanks the IISc Centenary Postdoctoral Fellowship for support. We are grateful to V. Venkataraman, Nigel Cooper, and Peter Littlewood for useful discussions.

*aamir@physics.iisc.ernet.in

¹R. Xu, A. Husmann, T. F. Rosenbaum, M. Saboungi, J. E. Enderby, and P. B. Littlewood, *Nature (London)* **390**, 57 (1997).

²M. P. Delmo, S. Yamamoto, S. Kasai, T. Ono, and K. Kobayashi, *Nature (London)* **457**, 1112 (2009).

³J. Hu and T. Rosenbaum, *Nat. Mater.* **7**, 697 (2008).

⁴M. M. Parish and P. B. Littlewood, *Nature (London)* **58**, 162 (2003).

⁵A. A. Abrikosov, *Phys. Rev. B* **58**, 2788 (1998).

⁶A. A. Abrikosov, *Phys. Rev. B* **60**, 4231 (1999).

⁷A. L. Friedman, J. L. Tedesco, P. M. Campbell, J. C. Culbertson, E. Aifer, F. K. Perkins, R. L. Myers-Ward, J. K. Hite, C. R. Eddy, G. G. Jernigan *et al.*, *Nano Lett.* **10**, 3962 (2010).

⁸H. He, B. Li, H. Liu, X. Guo, Z. Wang, M. Xie, and J. Wang, *Appl. Phys. Lett.* **100**, 032105 (2012).

- ⁹M. M. Parish and P. B. Littlewood, *Phys. Rev. B* **72**, 094417 (2005).
- ¹⁰M. Baenninger, A. Ghosh, M. Pepper, H. E. Beere, I. Farrer, P. Atkinson, and D. A. Ritchie, *Phys. Rev. B* **72**, 241311 (2005).
- ¹¹A. A. M. Staring, H. van Houten, C. W. J. Beenakker, and C. T. Foxon, *Phys. Rev. B* **45**, 9222 (1992).
- ¹²V. Tripathi and M. P. Kennett, *Phys. Rev. B* **74**, 195334 (2006).
- ¹³V. Tripathi and M. P. Kennett, *Phys. Rev. B* **76**, 115321 (2007).
- ¹⁴D. Neilson and A. R. Hamilton, *Phys. Rev. B* **82**, 035310 (2010).
- ¹⁵A. Ghosh, M. Pepper, H. E. Beere, and D. A. Ritchie, *J. Phys.: Condens. Matter* **16**, 3623 (2004).
- ¹⁶See Supplemental Material at <http://link.aps.org/supplemental/10.1103/PhysRevB.86.081203> for detailed analysis of I - V_{sd} curves, MR in other similar devices and its dependence on V_{sd} , and alternate theoretical description of NLMR.
- ¹⁷J. J. H. M. Schoonus, F. L. Bloom, W. Wagemans, H. J. M. Swagten, and B. Koopmans, *Phys. Rev. Lett.* **100**, 127202 (2008).
- ¹⁸Z. G. Sun, M. Mizuguchi, T. Manago, and H. Akinaga, *Appl. Phys. Lett.* **85**, 5643 (2004).
- ¹⁹C. Ciccarelli, B. G. Park, S. Ogawa, A. J. Ferguson, and J. Wunderlich, *Appl. Phys. Lett.* **97**, 082106 (2010).
- ²⁰C. I. Duruöz, R. M. Clarke, C. M. Marcus, and J. S. Harris, Jr., *Phys. Rev. Lett.* **74**, 3237 (1995).
- ²¹A. J. Rimberg, T. R. Ho, and J. Clarke, *Phys. Rev. Lett.* **74**, 4714 (1995).
- ²²R. Parthasarathy, X.-M. Lin, and H. M. Jaeger, *Phys. Rev. Lett.* **87**, 186807 (2001).
- ²³R. Parthasarathy, X.-M. Lin, K. Elteto, T. F. Rosenbaum, and H. M. Jaeger, *Phys. Rev. Lett.* **92**, 076801 (2004).
- ²⁴C. Reichhardt and C. J. Olson Reichhardt, *Phys. Rev. Lett.* **90**, 046802 (2003).
- ²⁵S. Goswami, M. A. Aamir, C. Siegert, M. Pepper, I. Farrer, D. A. Ritchie, and A. Ghosh, *Phys. Rev. B* **85**, 075427 (2012).
- ²⁶A. A. Middleton and N. S. Wingreen, *Phys. Rev. Lett.* **71**, 3198 (1993).
- ²⁷C. Herring, *J. Appl. Phys.* **31**, 1939 (1960).
- ²⁸D. J. Bergman and D. G. Stroud, *Phys. Rev. B* **62**, 6603 (2000).
- ²⁹D. Stroud and F. P. Pan, *Phys. Rev. B* **13**, 1434 (1976).
- ³⁰V. Guttal and D. Stroud, *Phys. Rev. B* **71**, 201304 (2005).
- ³¹H. Stachowiak, *Physica* **45**, 481 (1970).
- ³²S. L. Bud'ko, P. C. Canfield, C. H. Mielke, and A. H. Lacerda, *Phys. Rev. B* **57**, 13624 (1998).
- ³³P. Kapitza, *Proc. R. Soc. London, Ser. A* **119**, 358 (1928).
- ³⁴F. Y. Yang, K. Liu, K. Hong, D. H. Reich, P. C. Searson, and C. L. Chien, *Science* **284**, 1335 (1999).
- ³⁵P. Kapitza, *Proc. R. Soc. London, Ser. A* **123**, 292 (1929).
- ³⁶H. G. Johnson, S. P. Bennett, R. Barua, L. H. Lewis, and D. Heiman, *Phys. Rev. B* **82**, 085202 (2010).
- ³⁷Y. Meir, *Phys. Rev. Lett.* **83**, 3506 (1999).